Dykes as physical buffers to metamorphic overprinting: an example from the Archaean-Palaeoproterozoic Lewisian Gneiss Complex of Northwest Scotland

J. M. MACDONALD[1, *], C. MAGEE[2] AND K. M. GOODENOUGH[3]

[1]*Department of Earth, Ocean & Ecological Sciences, University of Liverpool, Liverpool, L69 3GP, UK*

[2]*Department of Earth Science & Engineering, Imperial College London, London, SW7 2AZ, UK*

[3]*British Geological Survey, Research Avenue South, Edinburgh, EH14 4AP, UK*

[*]*Present address: School of Geographical & Earth Sciences, University of Glasgow, Glasgow, G12 8QQ, UK.* *john.macdonald.3@glasgow.ac.uk*

Running header: "Dykes as physical buffers to metamorphic overprinting"

ABSTRACT

The early history of polymetamorphic basement gneiss complexes is often difficult to decipher due to overprinting by later deformation and metamorphic events. In this paper, we integrate field, petrographic and mineral chemistry data from an Archaean tonalitic gneiss xenolith, hosted within a Palaeoproterozoic mafic dyke in the Lewisian Gneiss Complex of NW Scotland to show how xenoliths in dykes may preserve signatures of early tectonothermal events. The Archaean tonalite-trondhjemite-granodiorite (TTG) gneisses of the Lewisian Gneiss Complex are cut by a suite of Palaeoproterozoic (~2400 Ma) mafic dykes, the Scourie Dyke Swarm, and both are deformed by later shear zones developed during the upper greenschist- to lower amphibolite-facies Laxfordian event (1740-1670 Ma). Detailed field mapping, petrographic analysis and mineral chemistry reveal that a xenolith of TTG gneiss entrained within a Scourie Dyke has been protected from amphibolite-facies recrystallization in a Laxfordian shear zone. Whereas the surrounding TTG gneiss displays pervasive amphibolite-facies retrogression, the xenolith retains a pre-Scourie Dyke, clinopyroxene-bearing metamorphic assemblage and gneissic layering. We suggest that retrogressive reaction softening and pre-existing planes of weakness, such as the ~2490 Ma Inverian fabric and gneiss-dyke contacts, localised strain around but not within the xenolith. Such strain localisation could generate preferential flow pathways for fluids, principally along the shear zone, bypassing the xenolith and protecting it from amphibolite-facies retrogression. In basement gneiss complexes where early metamorphic assemblages and fabrics have been fully overprinted by tectonothermal events, our results suggest that country rock xenoliths in mafic dykes could preserve windows into the early evolution of these complex polymetamorphic areas.

Key words: metamorphic overprinting; mafic dyke; buffer; TTG gneiss; xenolith

INTRODUCTION

Unravelling the geological history of polymetamorphic basement gneiss complexes is often difficult because mineral fabrics and metamorphic assemblages formed in older tectonothermal events are commonly overprinted by those formed during younger metamorphism and deformation (e.g. Holdsworth et al. 2001). Thermal disturbance can also reset isotopic and trace element signatures in petrogenetic indicator minerals such as zircon (e.g. Hoskin and Schaltegger 2003). These processes may therefore obscure our understanding of early tectonothermal events. However, complete overprinting does not always occur. For example, phenomena such as reaction softening and strain localisation can result in spatially heterogeneous tectonothermal overprinting (e.g. Oliot et al. 2010; White 2004). This is because structures generated by reaction softening and strain localisation (e.g. shear zones) may channel fluid flow, which is generally required to promote retrograde metamorphic reactions (e.g. White and Knipe 1978).

To investigate potential controls on heterogeneous overprinting, we present field, petrographic and geochemical evidence from the polymetamorphic tonalite-trondhjemite-granodiorite (TTG) Archaean gneisses of the Lewisian Gneiss Complex of Northwest Scotland (Fig. 1a). This work suggests that igneous intrusions may impede post-entrainment metamorphism and deformation of gneissic country rock xenoliths. In the Assynt Terrane (Kinny et al. 2005) of the Lewisian Gneiss Complex (Fig. 1a), the location of this study, field evidence shows that the TTG gneisses have undergone three tectonothermal events: (i) initial granulite-facies metamorphism with formation of gneissic layering (the Badcallian event); (ii) an amphibolite-facies metamorphism with formation of shear zones several kilometres wide (the Inverian event) followed by mafic dyke intrusion and hydrothermal activity; and (iii) a final episode of amphibolite-facies metamorphism with formation of shear zones tens of metres wide (the Laxfordian event) (e.g. Evans 1965; Park 1970; Sutton and Watson 1951; Wynn 1995). We examine a TTG xenolith within a Scourie Dyke that is characterised by an early gneissic layering and pyroxene-bearing mineral assemblage, despite

being entrained within a dyke that is deformed and metamorphosed by a shear zone formed during the Laxfordian event.

GEOLOGICAL SETTING

The Archaean-Palaeoproterozoic Lewisian Gneiss Complex, located in Northwest Scotland (Fig. 1a), is predominantly composed of tonalite-trondhjemite-granodiorite (TTG) gneiss, with abundant small bodies of mafic gneiss and sparse larger mafic bodies associated with metasedimentary gneisses (e.g. Johnson et al. 2016; Peach et al. 1907; Tarney and Weaver 1987). Early mapping of structures and metamorphic mineral assemblages by Sutton and Watson (1951) led to the recognition of two tectonothermal events, temporally separated by the emplacement of a suite of mafic dykes known as the Scourie Dyke Swarm. U-Pb dating has shown that while much of the Scourie dyke emplacement occurred at ~2400 Ma, there was also emplacement at ~2000 Ma (Davies and Heaman 2014). These pulses of dyke emplacement were separated by a hydrothermal event at ~2250 Ma which resulted in quartz-pyrite veins forming in many parts of the Assynt and Gruinard (Friend and Kinny 2001) terranes (Vernon et al. 2014). Subsequent work has shown that the pre-dyke tectonothermal event can be subdivided into a gneiss-forming, granulite-facies event (the Badcallian; Park 1970) and a younger amphibolite-facies event (the Inverian; Evans 1965). The Badcallian event is characterised by a gneissic layering and a rarely-preserved granulite-facies assemblage of plagioclase, clinopyroxene, orthopyroxene and quartz in the TTG gneisses. Widespread partial melting has also been shown to have occurred at this time (Johnson et al. 2013; Johnson et al. 2012). There has been much debate over the age of the Badcallian tectonothermal event (Crowley et al. 2015; Friend and Kinny 1995; Park 2005) but it is now generally accepted to have occurred at ~2700 Ma (Crowley et al. 2015). A major fluid influx during the ~2490 Ma (Crowley et al. 2015) Inverian tectonothermal event resulted in widespread hydrous retrogression of Badcallian pyroxenes to hornblende. Major shear zones up to ten kilometres wide were formed,

such as the Laxford Shear Zone (Goodenough et al. 2010) (Fig. 1b), while the areas between these major shear zones underwent partial static retrogression (e.g. Beach 1974).

Both the Badcallian and Inverian are heterogeneously overprinted by a post-Scourie dyke tectonothermal event, the Laxfordian, and their associated mineral assemblages and structures are only preserved in certain areas of the complex, most notably the Assynt Terrane (Fig. 1b) (Kinny et al. 2005). Throughout much of the Lewisian Gneiss Complex, the Laxfordian is characterised by pervasive deformation at upper greenschist to lower amphibolite facies (e.g. Park et al. 1987; Sutton and Watson 1951). In contrast, the Laxfordian event in the Assynt Terrane is represented by numerous discrete tens-of-metres-wide shear zones (e.g. MacDonald et al. 2015b; MacDonald et al. 2013; Wynn 1995) dated at c. 1740 Ma and 1670 Ma (Kinny et al. 2005), as well as extension-related alkaline granite sheets at c. 1880 Ma and compression/partial melting granite sheets at c. 1770 Ma (Goodenough et al. 2013). Because of the localised nature of Laxfordian deformation, metamorphic assemblages and deformation fabrics of the earlier Badcallian and Inverian tectonothermal events are locally preserved between Laxfordian shear zones.

RESULTS

FIELD RELATIONSHIPS

The field area for this study is located to the north of Loch a' Phreasain Challtuinne (NC 188 467; British National Grid) (Fig. 1c). This locality is within the Laxford Shear Zone, a ~5 km-wide shear zone formed during the Inverian tectonothermal event and reactivated during the Laxfordian tectonothermal event as multiple smaller shear zones that are tens of metres wide (Goodenough et al. 2010 and references therein). The margin of the Laxford Shear Zone is marked by a change from the Badcallian gneissic layering of the country rock to a steeply dipping, planar Inverian layering. The nearest pristine pyroxene-bearing granulite-facies Badcallian gneisses are located several kilometres to the southwest of the study area around Scourie (e.g. Johnson and White 2011; MacDonald et al.

2015a; Sutton and Watson 1951). We conducted detailed mapping of a small part of the Laxford Shear Zone that illustrates the polyphase deformation history of the area.

At the studied locality, a broadly north-south oriented, relatively planar Scourie Dyke, ~50 m wide, cross-cuts layering in the TTG gneiss at angles of up to 90° (e.g., NC18919 46689 and NC 18906 46735; Fig. 2). The layering in the TTG gneiss is characterised by fine (~5-10 mm thick), alternating layers of felsic and mafic minerals dipping at *c.* 70° to the SW. Weak mineral aggregate lineations of hornblende or quartz are also sparsely developed in the TTG gneiss. Both the planar and linear fabrics here are considered to be Inverian in age as they are associated with pyroxene-free amphibolite-facies mineralogy, but are cross-cut by the Scourie Dyke (Fig. 3a) and are located within the Inverian section of the Laxford Shear Zone mapped by Goodenough et al. (2010). The dyke is coarse-grained and composed of equant hornblende crystals with interstitial plagioclase (Fig. 3b).

Around NC 1889 4675, the dyke is deflected into a WNW-ESE orientation and deformed by a narrow Laxfordian shear zone (Fig. 2). A strong fabric of plagioclase aggregates is developed within the dyke (Fig. 3c), parallel to the planar fabric in the TTG gneisses. Within this narrow Laxfordian shear zone, layering in the gneisses is flaggy (Fig. 3d) with quartz and plagioclase aggregate lineations plunging at *c.* 5° WNW. The dyke contains discrete zones with a well-developed L-S tectonite fabric (e.g., NC 18838 46814; Fig. 3c), defined by aggregates of amphibole and/or plagioclase, clearly distinguishable from the tectonically undeformed dyke outside the Laxfordian shear zone. The dip and strike of the planar fabric is subparallel to the dyke-contact and dips >40° to the southwest. The transition in fabric style within the dyke is gradational over approximately 5 m and is characterised by the progressive elongation of anhedral, interstitial plagioclase into a zone where both hornblende and plagioclase form a strong L-S tectonite fabric (Fig. 3c&e). The offset of the dyke across the shear zone is sinistral with the variably plunging mineral lineation indicating a moderate degree of strike-slip movement at this locality. In the TTG gneisses, both the Inverian and Laxfordian planar fabrics dip at *c.* 60-70° to the southwest, suggesting Laxfordian deformation reactivated the earlier Inverian fabric.

Where the dyke is displaced by the Laxfordian shear zone, it contains four xenolithic masses of TTG gneiss (Fig. 2). These bodies are referred to as xenoliths because they do not have the same Inverian amphibolite-facies metamorphic assemblage as the country rock surrounding the dyke. The largest and southernmost of these xenoliths has an elliptical plan-view morphology and is *c.* 60 × 15 m in size with its long axis parallel to the dyke margins. Around this xenolith the Scourie Dyke displays a Laxfordian L-S tectonite fabric. However, only the outermost *c*. 1 m of the TTG gneiss xenolith has a dyke-contact parallel flaggy fabric (Fig. 3f), interpreted to be Laxfordian. The majority of the xenolith contains moderately well-developed gneissic layering which is defined by 5-20 mm wide layers of mafic and felsic minerals, consistent with Badcallian gneissic layering (Fig. 3f); clinopyroxene – not found in any of the other samples from this locality – is abundant. This TTG gneiss xenolith enclosed within the Scourie Dyke, and appears to have been transported to its current location and largely escaped overprinting, despite its position in a Laxfordian shear zone. In order to investigate this further, samples (cut normal to the foliation and parallel to the local lineation) for petrographic and mineral chemistry analysis were collected from the: (i) xenolith; (ii) deformed and (iii) undeformed Scourie Dyke; (iv) TTG gneiss in the Laxfordian shear zone; and (v) TTG gneiss outwith the Laxfordian shear zone but carrying an Inverian planar fabric.

PETROGRAPHY

Sample JM08/32 (NC 18904 46681) – TTG gneiss with Inverian fabric

Sample JM08/32 is composed of *c*. 50% quartz, *c*. 30% plagioclase, *c*. 10% hornblende, and *c*. 10% biotite. Accessory opaque minerals are commonly spatially associated with biotite. The plagioclase crystals are subhedral, up to 2 mm long, with occasional lamellar twinning and zoned extinction. The quartz crystals are up to 0.5 mm in diameter and locally aggregate to form a lineation (Fig. 4a). Hornblende occurs together with quartz in a sieve texture, suggesting it has replaced pyroxene (Pearce and Wheeler 2014). In places these pseudomorphs are elongate parallel to the quartz aggregate lineation (Fig. 4b). Biotite laths are commonly clumped together but only very weakly

179 align with the quartz fabric (Fig. 4c). The quartz aggregate lineation and elongated hornblende and
180 quartz pseudomorphs were formed during the Inverian event (Coward and Park 1987; Goodenough
181 et al. 2010).
182
183 **Sample JM08/28 (NC 18919 46696) – Undeformed Scourie Dyke**
184 Sample JM08/28 is composed of *c*. 65% hornblende, *c*. 30% plagioclase and *c*. 5% quartz with
185 accessory opaque minerals. The hornblende occurs dominantly in a sieve texture with quartz,
186 indicating replacement of igneous pyroxene. These pseudomorphs are generally *c.* 2 mm in diameter
187 and have rims of hornblende aggregates with hornblende containing numerous sub-millimetre
188 rounded quartz inclusions in its core (Fig. 4d). Clinopyroxene cores are locally preserved within the
189 pseudomorphs. Plagioclase forms 1-2 mm subhedral-to-anhedral crystals with well-preserved albite-
190 pericline lamellar twinning and zoned extinction (Fig. 4e). As well as occurring in a sieve texture with
191 hornblende, minor sub-millimetre anhedral quartz crystals are also found in the matrix. The lack of
192 any planar or linear fabrics show that this sample of Scourie Dyke has not been deformed but the
193 sieve-textured hornblende and quartz replacing igneous pyroxene demonstrates that it has been
194 statically retrogressed during the Laxfordian.
195
196 **Sample JM09/DC01 (NC 18959 46752) – TTG gneiss in the Laxfordian shear zone along strike from**
197 **the Scourie Dyke**
198 Sample JM09/DC01 is composed of *c*. 55% plagioclase, *c*. 25% quartz, *c*. 15% hornblende and *c*. 5%
199 biotite. Plagioclase crystals are subhedral, equant and 0.5-1 mm in diameter. They are thoroughly
200 sericitised and lamellar twinning and zoning are only rarely preserved. Quartz crystals are subhedral,
201 equant and 0.1-0.5 mm in diameter. They commonly aggregate to form a strong lineation (Fig. 4f).
202 Hornblende and biotite are also moderately aligned and parallel to this lineation.
203
204 **Sample JM08/29 (NC 18919 46758) – Deformed Scourie Dyke**

Sample JM08/29 is composed of *c*. 80% hornblende, *c*. 15% plagioclase and *c*. 5% clinopyroxene with accessory opaques. Hornblende crystals range from subhedral elongate to anhedral rounded shapes, 0.2-1 mm in diameter, which aggregate together to define a lineation (Fig. 4g). The pleochroic colour change occurs at the same angle in most crystals indicating that they grew during deformation. Plagioclase crystals are sub-millimetre in diameter and have an anhedral rounded shape. The clinopyroxene occurs in elongate lenses aligned with the hornblende fabric. The pyroxenes have a speckly altered appearance, occasionally pale-green in colour (Fig. 4h) with pink or blue birefringence. They have a reaction rim of equant plagioclase crystals which generally have well-defined concentric extinction. The clinopyroxenes are interpreted to be relict igneous crystals which were partially buffered from retrogression and deformation by their rims of plagioclase.

Sample JM08/30 (NC 18905 46760) – TTG gneiss from xenolith in Scourie Dyke

Sample JM08/30 is composed of *c*. 40% plagioclase, *c*. 25% clinopyroxene, *c*. 20% quartz and *c*. 15% hornblende. There is a compositional layering of mafic and felsic minerals at the thin section scale as well as at the hand specimen scale but no lineation. The plagioclase crystals are subhedral and generally equant, 0.5-2 mm in diameter; lamellar twinning and zoned extinction are commonly preserved. Quartz crystals have anhedral irregular shapes and are 0.1-1 mm in size. Both quartz and plagioclase have lobate grain boundaries (Fig. 4i). Clinopyroxene crystals are typically aggregated together in mafic bands and are pale green in colour with one prominent cleavage (Fig. 4j). They are equant and 1-2 mm across with reaction rims of aggregated equant sub-millimetre hornblende crystals. These rims are less than 1 mm wide and the hornblende is locally associated with very small quartz blebs (Fig. 4k); some clinopyroxenes have virtually no reaction rim and are in textural equilibrium with adjacent plagioclase (Fig. 4l). The reaction rims record minor retrogression to amphibolite-facies. Retrogression in this sample has been minor and of a much lesser degree than in the four other samples.

MINERAL CHEMISTRY

In order to quantify the chemical changes that occurred with chemical reactions during the different tectonothermal events indicated by petrographic observations, major element mineral chemistry was conducted. Si, Ti, Fe, Al, Mn, Mg, Ca, Na, K and Ti oxides were measured using a Cameca SX100 electron microprobe at the Natural History Museum, London. Operating conditions were 15 kV accelerating voltage, a specimen current of 20 nA and a spot size of 1 micron. Silicate or oxide standards were used, apart from for K for which a potassium bromide standard was used. Detection limits were ~0.02-0.05 oxide weight percent. Full data are given in the Supplementary Data; negligible core to rim zoning was observed and hence average values for each mineral are given in Table 1.

Hornblende and plagioclase in the Scourie dyke samples JM08/28 and JM08/29 both recrystallised during the Laxfordian tectonothermal event, although they are texturally different. The abundance of Na_2O and CaO in plagioclase is almost identical in the two samples and major element oxides in hornblende are also similar (Fig. 5, Table 1). Plagioclase in the TTG gneiss samples is much more sodic and less calcic (X_{An} = 0.29) than in the Scourie Dyke samples (X_{An} = 0.44). Plagioclase in the xenolith (sample JM08/30) is slightly more calcic and less sodic (X_{An} = 0.31-0.33) than those in the Inverian or Laxfordian assemblages (X_{An} = 0.29; Fig. 5, Table 1). Clinopyroxenes in the xenolith have low K_2O (<0.1 wt.%), but the narrow hornblende trims around them have higher K_2O (~1.3-1.5 wt.%) than the Laxfordian shear zone hornblendes and significantly higher K_2O than Inverian shear zone hornblendes (~0.8 wt.%). TiO_2 shows a similar pattern between samples than K_2O (Fig. 5, Table 1). Sieve-textured hornblende from the Inverian TTG gneiss is more silicic (~43.5 wt.%) than narrow hornblende rims around clinopyroxene in the xenolith (~41-43 wt.%) and hornblende laths recrystallized in the Laxfordian shear zone (42 wt.%).

DISCUSSION

The TTG gneiss xenolith contains a weak gneissic layering and equant clinopyroxenes with small retrogression rims of hornblende. The presence of clinopyroxene clearly distinguishes it from the Inverian and Laxfordian metamorphic assemblages observed in the surrounding TTG gneiss and suggests higher-grade metamorphism than the adjacent rocks. No orthopyroxene was found in thin section in this sample, so it is not strictly granulite-facies. However, orthopyroxene is very rare in Lewisian TTG gneisses and we interpret the mineral assemblage of the xenolith to be high-grade Badcallian. Additionally, the lobate grain boundaries between quartz and plagioclase is indicative of high-temperature grain boundary migration, often associated with deformation and recrystallisation at granulite-facies conditions (e.g. Passchier and Trouw 2005; Urai et al. 1986). The presence of narrow hornblende rims suggests that relatively minor amphibolite-facies retrogression has occurred within the xenolith. Overall, the xenolith mineral assemblage contrasts with the TTG gneiss host rock adjacent to the Scourie Dyke, which displays evidence of pervasive overprinting by tectonothermal events. This is demonstrated by: (i) a planar fabric and the absence of pyroxene in the Inverian shear zone (sample JM08/32), whereby original pyroxene has been completely retrogressed to sieve-textured hornblende and quartz (e.g. Beach 1974); (ii) the depletion of K and Ti in hornblende within sample JM08/32, relative to the minor hornblende rims in the xenolith (Fig. 5c & f; and (iii) sericitised feldspars and the development of planar and linear fabrics in sample JM09/DC01 consistent with its position within the Laxfordian shear zone (e.g. Sheraton et al. 1973). The enrichment of Ti and K in hornblende in the Laxfordian shear zone sample is attributed to an influx of Ti- and K-rich fluids during the Laxfordian, consistent with granite formation within and adjacent to the Laxford Shear Zone associated with partial melting of local crust (Goodenough et al. 2013; Goodenough et al. 2010). It is important to note that only the outer *c*. 1 m of the TTG xenolith displays a contact-parallel flaggy fabric.

Xenolith source and transportation

How did the Badcallian xenolith attain its current position in the Scourie Dyke in the Inverian- and Laxfordian- age Laxford Shear Zone? One explanation is that it is in-situ and a low-strain lacuna within the Inverian-age Laxford Shear Zone, which has been enveloped by the Scourie Dyke. However, the proximity of its current location to Inverian deformation would suggest that even if the xenolith had not been deformed during the Inverian, fluids circulating through the rocks would likely have completely retrogressed its Badcallian assemblage. Badcallian gneisses that have been statically retrogressed by Inverian fluids have very distinctive sieve-textured hornblende and quartz pseudomorphs after pyroxene (e.g. MacDonald et al. 2015a), something not observed in the xenolith, but seen widely outside the Laxfordian shear zone. As a result, we favour the interpretation that the xenolith was entrained and transported (for a distance of >~1 km) by the NE-SW oriented Scourie dyke from a position within the Badcallian TTG gneiss in the Assynt Terrane to the southwest of its current location (Figs. 1b & 6). We favour this source position because: (i) no TTG gneisses with Badcallian pyroxene-bearing assemblages are found to the northeast of the xenolith locality (Fig. 1b) (e.g. Beach 1974; Cohen et al. 1991; Whitehouse and Kemp 2010); and (ii) the TTG gneisses below the outcrop are still expected to lie within the steeply southwest-dipping Inverian-age Laxford Shear Zone. This model therefore implies that dyke emplacement involved a significant proportion of lateral, northwards-directed flow. Given that the xenolith is longer than the thickness (~50 m) of the dyke, it is probable that it was transported with its long axis oriented NW-SE, parallel to the dyke margins. During Laxfordian shearing, the Scourie dyke was deflected sinistrally and developed a Laxfordian fabric. Only the outer margins of the xenolith exhibit such a fabric and therefore underwent limited recrystallisation during Laxfordian shearing. The core of the xenolith was not recrystallised during the Laxfordian shearing and was simply rotated anticlockwise to a WNW-ESE orientation.

Post-emplacement dyke and xenolith evolution

309 Our observations indicate that the Scourie Dyke and the TTG gneiss host rocks in and around the
310 Laxfordian shear zone were retrogressed to amphibolite-facies during the Laxfordian tectonothermal
311 event. This is supported by: (i) the hornblende aggregate lineation in the Scourie Dyke, which
312 unequivocally shows that it was deformed and retrogressed in the Laxfordian shear zone; (ii) static
313 retrogression of igneous pyroxene to hornblende and quartz, which demonstrates that the dyke was
314 also affected by the Laxfordian thermal regime and fluid ingress beyond the shear zone; (iii) the
315 complete recrystallisation at amphibolite-facies of the TTG gneiss outside the dyke in both the
316 Inverian and Laxfordian parts of the shear zone; and (iv) narrow hornblende rims around the
317 xenolith clinopyroxenes are closer in their chemistry, particularly Ti and K, to Laxfordian shear zone
318 hornblende than Inverian shear zone hornblende. These chemical, mineralogical and textural
319 modifications observed in both the Scourie dyke and the TTG gneiss host rock suggest that H_2O-rich
320 fluids circulated through these rocks during the Laxfordian shear zone formation.
321 In contrast to those samples obtained from the Scourie dyke or the TTG gneiss host rock, our
322 results imply that the TTG gneiss xenolith was largely protected from retrogression and
323 recrystallization during the Laxfordian. This is supported by: (i) the preservation of a pyroxene-
324 bearing assemblage in the TTG gneiss xenolith; (ii) the limited development of hornblende rims
325 around pyroxenes in the xenolith; and (iii) the restriction of deformation fabrics to the outer margin
326 of the xenolith. To explain this localized heterogeneity in the distribution of amphibolite-facies
327 retrogression during the Laxfordian, we invoke a model whereby preferential metamorphism,
328 reaction softening and strain localisation in the dyke restricted xenolith-fluid interactions.
329 We suggest that during the initial influx of fluid in the Laxfordian, likely coincident with the
330 formation of the Laxfordian shear zone (e.g. Beach 1976), pyroxenes in both the Scourie Dyke and
331 the TTG gneiss xenolith started to undergo retrogression. This could explain the formation of small
332 hornblende rims on pyroxenes in the xenolith and the development of a contact-parallel fabric in the
333 outer margin of the xenolith generated by the onset of shear zone deformation. This hypothesis is
334 supported by the observation that that Ti and K concentrations in the narrow hornblende rims

around clinopyroxenes in the xenolith and in hornblendes from the Laxfordian shear zone are similar, but both higher than in the Inverian shear zone hornblendes. Because of the relatively large proportion of quartz, and plagioclase to a lesser extent, in the TTG gneiss xenolith compared to the Scourie Dyke, we suggest that the contemporaneous retrogression of both rock types progressed at a faster rate within the dyke; i.e. there was a greater amount of pyroxene available that could retrogress to hornblende. Importantly, these mineralogical and chemical changes from pyroxene to hornblende inevitably change the physical properties of the rock. The transformation can be considered to involve a form of reaction softening, where minerals such as hornblende are weaker. The formation of hornblende aggregates in sample JM09/DC01 (the Laxfordian shear zone) can instigate a mineral preferred orientation and thereby further weaken the rock. Plagioclase alteration to sericite (e.g., sample JM09/DC01), a much weaker phyllosilicate, also induces reaction softening. Additionally, many studies have documented that the occurrence of reaction softening processes in metamorphic rocks can focus strain (e.g. Holyoke and Tullis 2006a, b; Stünitz and Tullis 2001; White and Knipe 1978; Wibberley 1999), promoting the formation of shear zones (e.g. Keller et al. 2004; Oliot et al. 2010; Whitmeyer and Wintsch 2005).

We suggest that the greater propensity for retrogression of pyroxene to amphibole in the Scourie Dyke, compared to the more felsic TTG gneiss xenolith, would have resulted in more pronounced reaction softening and strain localisation in the dyke, leaving the gneiss xenolith relatively untouched. In conjunction with field and microstructural work demonstrating that the Scourie dykes accommodated more strain (and therefore deformed more) than the TTG gneisses (Pearce et al. 2011), this strain localisation may explain why strong planar and linear fabrics are developed in pervasively the dyke but only at the outer margins of the TTG gneiss xenolith. Similarly, Wheeler *et al*., (1987) showed that Laxfordian deformation was concentrated along dyke margins at Diabaig in the southern part of the mainland Lewisian Gneiss Complex outcrop. Park *et al*., (1987) suggested that as deformation progressed, strain initially localised at the dyke margins would start to affect the whole of the dyke. Strain localisation can control fluid flow and is here interpreted to

have been an important process in directing fluids around, but not through, the xenolith. This is consistent with previous studies, which have shown that the Laxfordian shear zones throughout the Lewisian Gneiss Complex acted as preferential fluid-flow pathways during the Laxfordian tectonothermal event (Beach 1973, 1976). Strain localisation leading to directed fluid flow is a common phenomenon and many examples are discussed in the literature (e.g. Babiker and Gudmundsson 2004; Blenkinsop and Kadzviti 2006; Clark et al. 2005; Goldblum and Hill 1992; Ring 1999; Tartese et al. 2012). For instance, Cartwright et al., (2001) showed that fluid flow during tectonothermal activity in the Reynolds Range, Australia, was channelled along shear zones or along distinct lithological contacts – very similar as the situation discussed in this paper. Similarly, blocks of anhydrous granulite-facies assemblages in the Western Gneiss region of Norway are preserved from fluid-induced amphibolite-facies retrogression or eclogitisation as these processes are focussed in shear zones where fluid flow has promoted metamorphic reactions which produce softer minerals, which then allow for strain localisation (e.g. Krabbendam et al. 2000). Several studies have similarly demonstrated that crystallised igneous intrusions may deflect migrating fluids along their margins, leaving their interiors relatively unaffected (Grove 2014; Jacquemyn et al. 2014; Rateau et al. 2013).The proposed model (Fig. 6) implies that the interplay between the processes of reaction softening, strain localisation (e.g., shear zone development) and directed fluid flow resulted in the xenolith escaping amphibolite-facies retrogression. This combination of factors allows the local preservation of early metamorphic assemblages and fabrics in polymetamorphic terranes, specifically in dyke-hosted country rock xenoliths.

CONCLUSIONS

This study illustrates an example of a mafic dyke acting as a physical barrier to metamorphic overprinting of entrained country rock xenoliths from the Archaean-Palaeoproterozoic Lewisian Gneiss Complex of Northwest Scotland. Field mapping and petrographic analysis show that a

tonalite-trondhjemite-granodiorite (TTG) gneiss xenolith entrained in a member of the Scourie Dyke Swarm retains a Badcallian pyroxene-bearing mineral assemblage and coarse gneissic layering without lineation, whereas the dyke and surrounding country rock display evidence of Inverian and Laxfordian amphibolite-facies overprinting that includes linear fabric elements. We suggest that the xenolith was entrained by the dyke from an area unaffected by the Inverian tectonothermal event, likely to the SW of the current exposure,. Mineral chemistry highlights some of the chemical changes that have occurred within the major minerals due to the influx of fluid that resulted in retrogressive metamorphic reactions. We interpret that the xenolith escaped Laxfordian retrogression through an interplay of factors: reaction softening, strain localisation and directed fluid flow. Retrogressive reaction softening, along with planes of weakness such as the pre-existing Inverian fabric and gneiss-dyke contacts, localised strain around but not within the xenolith. Strain localisation generated preferential flow pathways for fluids, principally along the shear zone. In the Lewisian Gneiss Complex, areas with early metamorphic assemblages and fabrics survive but in many polymetamorphic terranes this is not the case. This study shows that gneissic country rock xenoliths in mafic dykes could help to unravel polymetamorphic histories of basement gneiss complexes where the majority of the country rock has been overprinted, obscuring early tectonothermal events.

ACKNOWLEDGEMENTS

The fieldwork was carried out under UK Natural Environment Research Council DTG NE/G523855/1 and British Geological Survey CASE Studentship 2K08E010 to JMM. John Wheeler and Quentin Crowley assisted with fieldwork. Alan Boyle is thanked for taking the photomicrographs. John Spratt assisted with mineral chemistry analyses at the Natural History Museum. Maarten Krabbendam is thanked for editorial handling and Tim Johnson and Bob Holdsworth for detailed and constructive

reviews which considerably improved the manuscript. KG publishes with the permission of the Executive Director of the British Geological Survey.

Figure Captions

Fig. 1. Location maps. (a) Outcrop of the Lewisian Gneiss Complex in Northwest Scotland, inset map shows location in the wider British and Irish Isles. (b) Location of the locality investigated in this study relative to the major geological structure in the area, the Laxford Shear Zone. (c) detailed location map.

Fig. 2. Detailed field map of lithology and structure at the locality with sample locations marked. Inset equal area stereonet showing poles to planar fabrics and lineations; colours match main map.

Fig. 3. (a) Photograph showing undeformed Scourie dyke cross-cutting Inverian fabric in TTG gneiss; walking pole is 120 cm long. (b) Equant hornblende and plagioclase in undeformed Scourie dyke. (c) Photograph of strongly deformed Scourie dyke with inset sketch showing L-S tectonite nature of fabric. (d) Photograph showing Laxfordian deformation of TTG gneiss and Scourie dyke in Laxfordian shear zone; walking pole is 120 cm long. (e) Field sketch showing onset of deformation in the Scourie dyke at the margin of the Laxfordian shear zone with photographs of fabric styles, with photograph of weak plagioclase aggregate lineation in Scourie dyke. (f) Photograph of moderately-developed Badcallian layering in xenolith with flaggy Laxfordian fabric at xenolith margin in contact with deformed Scourie dyke; walking pole is 120 cm long.

Fig. 4. Photomicrographs of the samples analysed petrographically. (a) Quartz mineral aggregate lineation in sample JM08/32, TTG gneiss with Inverian fabric. (b) Elongate sieve-textured hornblende and quartz pseudomorphs after pyroxene in sample JM08/32. (c) Clumps of weakly aligned biotite laths, roughly aligned with the quartz aggregate lineation. (d) Pseudomorphs after pyroxene of sieve-textured hornblende and quartz in sample JM08/28, undeformed Scourie dyke; the edges of the pseudomorphs are dominated by hornblende with more quartz in the cores. (e) Plagioclase showing well-preserved lamellar twinning and zoned extinction in sample JM08/28. (f) Quartz

mineral aggregate lineation in sample JM09/DC01, TTG gneiss in the Laxfordian shear zone along strike from the Scourie dyke. (g) Hornblende crystals aggregated to form a strong lineation in sample JM08/29, the deformed Scourie dyke. (h) Elongate lenses of relict clinopyroxene in sample JM08/29. (i) White arrows denote lobate grain boundaries in quartz and plagioclase in sample JM08/30, TTG gneiss from xenolith in Scourie dyke. (j) Clinopyroxene crystals aggregated together in sample JM08/30, TTG gneiss from xenolith in Scourie dyke. (k) Clinopyroxene with rim of aggregated hornblende crystals in sample JM08/30. (l) Clinopyroxene with no hornblende rim in textural equilibrium with plagioclase in sample JM08/30.

Fig. 5. Plots of mineral chemistry data (in weight percentage cation oxide) from the samples analysed in this study. (a) Na vs CaO in plagioclase. (b) Mg vs Si in hornblende. (c) Ti vs Si in hornblende. (d) Na vs Si in hornblende. (e) Mn vs Si in hornblende. (f) K vs Si in hornblende.

Fig. 6. Schematic maps illustrating the tectonothermal evolution of the xenolith and surrounding rocks, not to scale.

Table Captions

Table 1. Mineral chemistry data. Cation oxide values in weight percent. Cation values in number of ions per formula unit; number of oxygens used in this calculation: hornblende = 23, clinpyroxene = 6, plagioclase = 8, biotite = 11. “plag” denotes plagioclase, “cpx” clinopyroxene, “bt” biotite and “hbl” hornblende.

REFERENCES

Babiker, M. & Gudmundsson, A. 2004. The effects of dykes and faults on groundwater flow in an arid land: the Red Sea Hills, Sudan. *Journal of Hydrology*, 297, 256-273.

Beach, A. 1973. Mineralogy of High-Temperature Shear Zones at Scourie, NW Scotland. *Journal of Petrology*, 14, 231-248.

Beach, A. 1974. Amphibolitization of Scourian granulites. *Scottish Journal of Geology*, 10, 35-43.

Beach, A. 1976. Interrelations of Fluid Transport, Deformation, Geochemistry and Heat-Flow in Early Proterozoic Shear Zones in Lewisian Complex. *Philosophical Transactions of the Royal Society of London Series a-Mathematical Physical and Engineering Sciences*, 280, 569-604.
Blenkinsop, T.G. & Kadzviti, S. 2006. Fluid flow in shear zones: insights from the geometry and evolution of ore bodies at Renco gold mine, Zimbabwe. *Geofluids*, 6, 334-345.
Cartwright, I., Buick, I.S. & Vry, J.K. 2001. Fluid-rock interaction in the Reynolds Range, central Australia: superimposed, episodic, and channelled fluid flow systems. *Geological Society, London, Special Publications*, 184, 357-379.
Clark, C., Mumm, A.S. & Faure, K. 2005. Timing and nature of fluid flow and alteration during Mesoproterozoic shear zone formation, Olary Domain, South Australia. *Journal of Metamorphic Geology*, 23, 147-164.
Cohen, A.S., Onions, R.K. & O' Hara, M.J. 1991. Chronology and Mechanism of Depletion in Lewisian Granulites. *Contributions to Mineralogy and Petrology*, 106, 142-153.
Coward, M. & Park, R.G. 1987. The role of mid-crustal shear zones in the Early Proterozoic evolution of the Lewisian. *In*: Park, R.G. & Tarney, J. (eds.) *Evolution of the Lewisian and Comparable Precambrian High-Grade Terrains*. Geological Society, London, Special Publication 27, 127-138.
Crowley, Q.G., Key, R. & Noble, S.R. 2015. High-precision U–Pb dating of complex zircon from the Lewisian Gneiss Complex of Scotland using an incremental CA-ID-TIMS approach. *Gondwana Research*, 27, 1381-1391.
Davies, J.H.F.L. & Heaman, L. 2014. New U-Pb baddeleyite and zircon ages for the Scourie dyke swarm: A long-lived large igneous province with implications for the Paleoproterozoic evolution of NW Scotland. *Precambrian Research*, 249, 180-198.
Evans, C.R. 1965. Geochronology of the Lewisian Basement near Lochinver, Sutherland. *Nature*, 204, 638-641.
Friend, C.R.L. & Kinny, P.D. 1995. New Evidence for Protolith Ages of Lewisian Granulites, Northwest Scotland. *Geology*, 23, 1027-1030.
Friend, C.R.L. & Kinny, P.D. 2001. A reappraisal of the Lewisian Gneiss Complex: geochronological evidence for its tectonic assembly from disparate terranes in the Proterozoic. *Contributions to Mineralogy and Petrology*, 142, 198-218.
Goldblum, D.R. & Hill, M.L. 1992. Enhanced Fluid-Flow Resulting from Competence Contrast within a Shear Zone - the Garnet Ore Zone at Gore Mountain, Ny. *Journal of Geology*, 100, 776-782.
Goodenough, K.M., Crowley, Q., Krabbendam, M. & Parry, S.F. 2013. New U-Pb age constraints for the Laxford Shear Zone, NW Scotland: evidence for tectono-magmatic processes associated with the formation of a Palaeoproterozoic supercontinent. *Precambrian Research*, 223, 1-19.
Goodenough, K.M., Park, R.G., Krabbendam, M., Myers, J.S., Wheeler, J., Loughlin, S.C., Crowley, Q.G., Friend, C.R.L., Beach, A., Kinny, P.D. & Graham, R.H. 2010. The Laxford Shear Zone: an end-Archaean terrane boundary? *In*: Law, R.D., Butler, R.W.H., Holdsworth, R.E., Krabbendam, M. & Strachan, R.A. (eds.) *Continental Tectonics and Mountain Building*. Geological Society, London, Special Publications 335, 103-120.
Grove, C. 2014. *Direct and Indirect Effects of Flood Basal Volcanism on Reservoir Quality Sandstone*Ph.D., Durham University.
Holdsworth, R.E., Hand, M., Miller, J.A. & Buick, I.S. 2001. Continental reactivation and reworking: an introduction. *In*: Miller, J.A., Holdsworth, R.E., Buick, I.S. & Hand, M. (eds.) *Continental reactivation and reworking* Geological Society, London184, 1-12.
Holyoke, C.W. & Tullis, J. 2006a. Formation and maintenance of shear zones. *Geology*, 34, 105-108.
Holyoke, C.W. & Tullis, J. 2006b. Mechanisms of weak phase interconnection and the effects of phase strength contrast on fabric development. *Journal of Structural Geology*, 28, 621-640.
Hoskin, P.W.O. & Schaltegger, U. 2003. The composition of zircon and igneous and metamorphic petrogenesis. *In*: Hanchar, J. & Hoskin, P.W.O. (eds.) *Zircon*. Mineralogical Society of America and The Geochemical Society, 27-62.

517 Jacquemyn, C., El Desouky, H., Hunt, D., Casini, G. & Swennen, R. 2014. Dolomitization of the
518 Latemar platform: Fluid flow and dolomite evolution. *Marine and petroleum geology*, 55, 43-67.
519 Johnson, T.E., Brown, M., Goodenough, K.M., Clark, C., Kinny, P.D. & White, R.W. 2016. Subduction
520 or sagduction? Ambiguity in constraining the origin of ultramafic–mafic bodies in the Archean crust
521 of NW Scotland. *Precambrian Research*, 283, 89-105.
522 Johnson, T.E., Fischer, S. & White, R.W. 2013. Field and petrographic evidence for partial melting of
523 TTG gneisses from the central region of the mainland Lewisian complex, NW Scotland. *Journal of the*
524 *Geological Society*, 170, 319-326.
525 Johnson, T.E., Fischer, S., White, R.W., Brown, M. & Rollinson, H.R. 2012. Archaean Intracrustal
526 Differentiation from Partial Melting of Metagabbro-Field and Geochemical Evidence from the
527 Central Region of the Lewisian Complex, NW Scotland. *Journal of Petrology*, 53, 2115-2138.
528 Johnson, T.E. & White, R.W. 2011. Phase equilibrium constraints on conditions of granulite-facies
529 metamorphism at Scourie, NW Scotland. *Journal of the Geological Society*, 168, 147-158.
530 Keller, L.M., Abart, R., Stünitz, H. & De Capitani, C. 2004. Deformation, mass transfer and mineral
531 reactions in an eclogite facies shear zone in a polymetamorphic metapelite (Monte Rosa nappe,
532 western Alps). *Journal of Metamorphic Geology*, 22, 97-118.
533 Kinny, P.D., Friend, C.R.L. & Love, G.J. 2005. Proposal for a terrane-based nomenclature for the
534 Lewisian Gneiss Complex of NW Scotland. *Journal of the Geological Society*, 162, 175-186.
535 Krabbendam, M., Wain, A. & Andersen, T.B. 2000. Pre-Caledonian granulite and gabbro enclaves in
536 the Western Gneiss Region, Norway: indications of incomplete transition at high pressure.
537 *Geological Magazine*, 137, 235-255.
538 MacDonald, J.M., Goodenough, K.M., Wheeler, J., Crowley, Q., Harley, S.L., Mariani, E. & Tatham, D.
539 2015a. Temperature–time evolution of the Assynt Terrane of the Lewisian Gneiss Complex of
540 Northwest Scotland from zircon U-Pb dating and Ti thermometry. *Precambrian Research*, 260, 55-75.
541 MacDonald, J.M., Goodenough, K.M., Wheeler, J., Crowley, Q., Harley, S.L., Mariani, E. & Tatham, D.
542 2015b. Temperature–time evolution of the Assynt Terrane of the LewisianGneiss Complex of
543 Northwest Scotland from zircon U-Pb dating and Tithermometry. *Precambrian Research*, 260, 55-75.
544 MacDonald, J.M., Wheeler, J., Harley, S.L., Mariani, E., Goodenough, K.M., Crowley, Q. & Tatham, D.
545 2013. Lattice distortion in a zircon population and its effects on trace element mobility and U–Th–Pb
546 isotope systematics: examples from the Lewisian Gneiss Complex, northwest Scotland. *Contributions*
547 *to Mineralogy and Petrology*, 166, 21-41.
548 Oliot, E., Goncalves, P. & Marquer, D. 2010. Role of plagioclase and reaction softening in a
549 metagranite shear zone at mid-crustal conditions (Gotthard Massif, Swiss Central Alps). *Journal of*
550 *Metamorphic Geology*, 28, 849-871.
551 Park, R.G. 1970. Observations on Lewisian Chronology. *Scottish Journal of Geology*, 6, 379-399.
552 Park, R.G. 2005. The Lewisian terrane model: a review. *Scottish Journal of Geology*, 41, 105-118.
553 Park, R.G., Crane, A. & Niamatullah, M. 1987. Early Proterozoic structure and kinematic evolution of
554 the southern mainland Lewisian. *In*: Park, R.G. & Tarney, J. (eds.) *Evolution of the Lewisian and*
555 *Comparable Precambrian High-Grade Terrains* 27, 139-152.
556 Passchier, C.W. & Trouw, R.A.J. 2005. Microtectonics. Springer-Verlag, Heidelberg.
557 Peach, B.N., Horne, J., Gunn, W., Clough, C.T. & Hinxman, L.W. 1907. The Geological Structure of the
558 Northwest Highlands of Scotland. H.M.S.O., London.
559 Pearce, M.A. & Wheeler, J. 2014. Microstructural and Metamorphic Constraints on the Thermal
560 Evolution of the Southern Region of the Lewisian Gneiss Complex, NW Scotland. *Journal of*
561 *Petrology*, 55, 2043-2066.
562 Pearce, M.A., Wheeler, J. & Prior, D.J. 2011. Relative strength of mafic and felsic rocks during
563 amphibolite facies metamorphism and deformation. *Journal of Structural Geology*, 33, 662-675.
564 Rateau, R., Schofield, N. & Smith, M. 2013. The potential role of igneous intrusions on hydrocarbon
565 migration, West of Shetland. *Petroleum Geoscience*, 19, 259-272.

566 Ring, U. 1999. Volume loss, fluid flow, and coaxial versus noncoaxial deformation in retrograde,
567 amphibolite facies shear zones, northern Malawi, east-central Africa. *Geological Society of America*
568 *Bulletin*, 111, 123-142.
569 Sheraton, J.W., Tarney, J., Wheatley, T.J. & Wright, A.E. 1973. The structural history of the Assynt
570 district. *In*: Park, R.G. & Tarney, J. (eds.) *The Early Precambrian of Scotland and Related Rocks of*
571 *Greenland*. University of Keele, 31-43.
572 Stünitz, H. & Tullis, J. 2001. Weakening and strain localization produced by syn-deformational
573 reaction of plagioclase. *International Journal of Earth Sciences*, 90, 136-148.
574 Sutton, J. & Watson, J. 1951. The pre-Torridonian metamorphic history of the Loch Torridon and
575 Scourie areas in the North-West Highlands, and its bearing on the chronological classification of the
576 Lewisian. *Quarterly Journal of the Geological Society*, 106, 241-296.
577 Tarney, J. & Weaver, B.L. 1987. Geochemistry of the Scourian Complex: petrogenesis and tectonic
578 models. *In*: Park, R.G. & Tarney, J. (eds.) *Evolution of the Lewisian and Comparable Precambrian*
579 *High-Grade Terrains* Geological Society, London27, 45-56.
580 Tartese, R., Boulvais, P., Poujol, M., Chevalier, T., Paquette, J.L., Ireland, T.R. & Deloule, E. 2012.
581 Mylonites of the South Armorican Shear Zone: Insights for crustal-scale fluid flow and water-rock
582 interaction processes. *Journal of Geodynamics*, 56-57, 86-107.
583 Urai, J., Means, W.D. & Lister, G.S. 1986. Dynamic Rrecrystallisation of Minerals. *In*: Heard, H.C. &
584 Hobbs, B.E. (eds.) *Mineral and rock deformation: laboratory studies, the Paterson volume*. American
585 Geophysical Union, Washington DC, 161-200.
586 Vernon, R., Holdsworth, R.E., Selby, D., Dempsey, E., Finlay, A.J. & Fallick, A.E. 2014. Structural
587 characteristics and Re–Os dating of quartz-pyrite veins in the Lewisian Gneiss Complex, NW
588 Scotland: Evidence of an Early Paleoproterozoic hydrothermal regime during terrane amalgamation.
589 *Precambrian Research*, 246, 256-267.
590 Wheeler, J., Windley, B.F. & Davies, F.B. 1987. Internal evolution of the major Precambrian shear
591 belt at Torridon, NW Scotland. *In*: Park, R.G. & Tarney, J. (eds.) *Evolution of the Lewisian and*
592 *Comparable Precambrian High-Grade Terrains* Geological Society, London27, 153-164.
593 White, J.C. 2004. Instability and localization of deformation in lower crust granulites, Minas fault
594 zone, Nova Scotia, Canada. *In*: Alsop, G.I., Holdsworth, R.E., McCaffrey, K.W. & Hand, M. (eds.) *Flow*
595 *Processes in Faults and Shear Zones*. Geological Society, London224, 25-37.
596 White, S.H. & Knipe, R.J. 1978. Transformation- and reaction-enhanced ductility in rocks. *Journal of*
597 *the Geological Society*, 135, 513-516.
598 Whitehouse, M. & Kemp, A.I.S. 2010. On the difficulty of assigning crustal residence, magmatic
599 protolith and metamorphic ages to Lewisian granulites: constraints from combined in-situ U-Pb and
600 Lu-Hf isotopes. *In*: Law, R.D., Butler, R.W.H., Holdsworth, R.E., Krabbendam, M. & Strachan, R.A.
601 (eds.) *Continental Tectonics and Mountain Building: The Legacy of Peach and Horne* Geological
602 Society, London, Special Publications 335, 81-101.
603 Whitmeyer, S.J. & Wintsch, R.P. 2005. Reaction localization and softening of texturally hardened
604 mylonites in a reactivated fault zone, central Argentina. *Journal of Metamorphic Geology*, 23, 411-
605 424.
606 Wibberley, C. 1999. Are feldspar-to-mica reactions necessarily reaction-softening processes in fault
607 zones? *Journal of Structural Geology*, 21, 1219-1227.
608 Wynn, T.J. 1995. Deformation in the mid to lower continental crust: analogues from Proterozoi shear
609 zones in NW Scotland. *In*: Coward, M.P. & Ries, A.C. (eds.) *Early Precambrian Processes* Geological
610 Society, London95, 225-241.

611

Sample	JM08/28			JM08/29	JM08/30		JM08/32	JM09/DC01	JM08/30				JM08/32
Mineral	plag	plag	plag	plag	plag	plag	plag	plag	cpx	cpx	cpx	cpx	bt
SiO_2	57.14	57.41	58.22	57.17	59.26	61.50	61.72	62.63	50.31	51.39	51.77	50.48	34.98
TiO_2	0.00	0.02	0.02	0.01	0.03	0.00	0.00	0.00	0.14	0.07	0.10	0.11	2.46
Al_2O_3	27.62	27.51	27.68	26.65	25.14	25.08	25.02	24.62	2.02	1.27	1.46	1.59	16.85
FeO	0.24	0.09	0.08	0.18	0.09	0.04	0.02	0.05	11.10	9.87	10.52	10.59	20.78
MnO	0.00	0.01	0.00	0.00	0.00	0.00	0.00	0.00	0.56	0.57	0.59	0.58	0.13
MgO	0.07	0.00	0.00	0.00	0.00	0.00	0.00	0.00	11.36	12.09	11.63	11.64	11.63
CaO	9.31	9.33	9.43	9.12	7.10	6.62	6.36	6.10	23.17	24.17	24.02	23.88	0.11
Na_2O	6.45	6.61	6.57	6.57	7.92	8.13	8.43	8.33	0.71	0.62	0.67	0.68	0.16
K_2O	0.24	0.07	0.07	0.07	0.23	0.24	0.06	0.10	0.10	0.00	0.01	0.02	6.93
Cr_2O_3	0.01	0.00	0.00	0.00	0.00	0.00	0.01	0.00	0.05	0.04	0.04	0.06	0.05
Total	101.09	101.08	102.07	99.77	99.77	101.62	101.64	101.85	99.56	100.14	100.87	99.68	94.32
Si	2.54	2.55	2.56	2.57	2.66	2.70	2.70	2.73	1.93	1.95	1.95	1.93	2.68
Ti	0.00	0.00	0.00	0.00	0.00	0.00	0.00	0.00	0.00	0.00	0.00	0.00	0.14
Al	1.45	1.44	1.43	1.41	1.33	1.30	1.29	1.26	0.09	0.06	0.06	0.07	1.52
Fe	0.01	0.00	0.00	0.01	0.00	0.00	0.00	0.00	0.36	0.31	0.33	0.34	1.33
Mn	0.00	0.00	0.00	0.00	0.00	0.00	0.00	0.00	0.02	0.02	0.02	0.02	0.01
Mg	0.00	0.00	0.00	0.00	0.00	0.00	0.00	0.00	0.65	0.68	0.65	0.66	1.33
Ca	0.44	0.44	0.44	0.44	0.34	0.31	0.30	0.28	0.95	0.98	0.97	0.98	0.01
Na	0.56	0.57	0.56	0.57	0.69	0.69	0.72	0.70	0.05	0.05	0.05	0.05	0.02
K	0.01	0.00	0.00	0.00	0.01	0.01	0.00	0.00	0.00	0.00	0.00	0.00	0.68
Cr	0.00	0.00	0.00	0.00	0.00	0.00	0.00	0.00	0.00	0.00	0.00	0.00	0.00
X_{Mg}									0.65	0.69	0.66	0.66	0.50
X_{An}	0.44	0.44	0.44	0.43	0.33	0.31	0.29	0.29					
Total Cations	5.01	5.01	5.00	5.00	5.03	5.01	5.01	4.99	4.05	4.04	4.03	4.05	7.73

Sample		JM08/28		JM08/29		JM08/30			JM08/32		JM09/DC01
Mineral	hbl	hbl	hbl	hbl	hbl	hbl	hbl	hbl	hbl	hbl	hbl
Texture	sieve-texture	sieve-texture	sieve-texture	rim around remnant cpx?	rim round cpx	rim round cpx	rim round cpx	rim round cpx	sieve-texture	sieve-texture	lath
SiO_2	42.75	41.64	45.31	42.39	40.85	42.90	41.55	40.77	43.68	43.52	41.97
TiO_2	0.89	0.77	0.48	0.77	0.78	0.64	0.77	0.79	0.29	0.54	0.94
Al_2O_3	11.05	12.42	9.46	12.63	11.49	9.84	12.11	11.38	11.23	11.12	11.63
FeO	18.85	20.44	18.30	18.53	19.73	18.30	18.29	19.82	17.51	17.70	18.33
MnO	0.33	0.32	0.31	0.29	0.44	0.45	0.45	0.46	0.34	0.31	0.30
MgO	9.15	7.86	10.19	8.77	8.72	9.31	9.07	8.66	10.27	9.94	9.56
CaO	11.94	11.74	12.18	11.33	12.10	13.02	12.16	12.14	11.91	11.89	11.94
Na_2O	1.54	1.57	1.19	1.61	1.34	1.19	1.38	1.30	1.27	1.32	1.47
K2O	0.45	0.61	0.37	0.57	1.44	1.32	1.53	1.47	0.78	0.81	1.22
Cr_2O_3	0.04	0.04	0.13	0.03	0.07	0.05	0.11	0.06	0.03	0.04	0.05
Total	97.22	97.64	98.12	97.23	97.07	97.10	97.51	96.96	97.45	97.33	97.69
Si	6.52	6.37	6.78	6.43	6.33	6.58	6.35	6.33	6.58	6.58	6.39
Ti	0.10	0.09	0.05	0.09	0.09	0.07	0.09	0.09	0.03	0.06	0.11
Al	1.98	2.24	1.67	2.26	2.10	1.78	2.18	2.08	2.00	1.98	2.09
Fe	2.40	2.62	2.29	2.35	2.56	2.35	2.34	2.57	2.21	2.24	2.33
Mn	0.04	0.04	0.04	0.04	0.06	0.06	0.06	0.06	0.04	0.04	0.04
Mg	2.08	1.79	2.28	1.98	2.01	2.13	2.07	2.00	2.31	2.24	2.17
Ca	1.95	1.92	1.95	1.84	2.01	2.14	1.99	2.02	1.92	1.93	1.95
Na	0.46	0.47	0.35	0.47	0.40	0.35	0.41	0.39	0.37	0.39	0.43
K	0.09	0.12	0.07	0.11	0.29	0.26	0.30	0.29	0.15	0.16	0.24
Cr	0.00	0.00	0.02	0.00	0.01	0.01	0.01	0.01	0.00	0.00	0.01
X_{Mg}	0.46	0.41	0.50	0.46	0.44	0.48	0.47	0.44	0.51	0.50	0.48
Total Cations	15.62	15.67	15.50	15.59	15.85	15.73	15.79	15.85	15.62	15.61	15.74

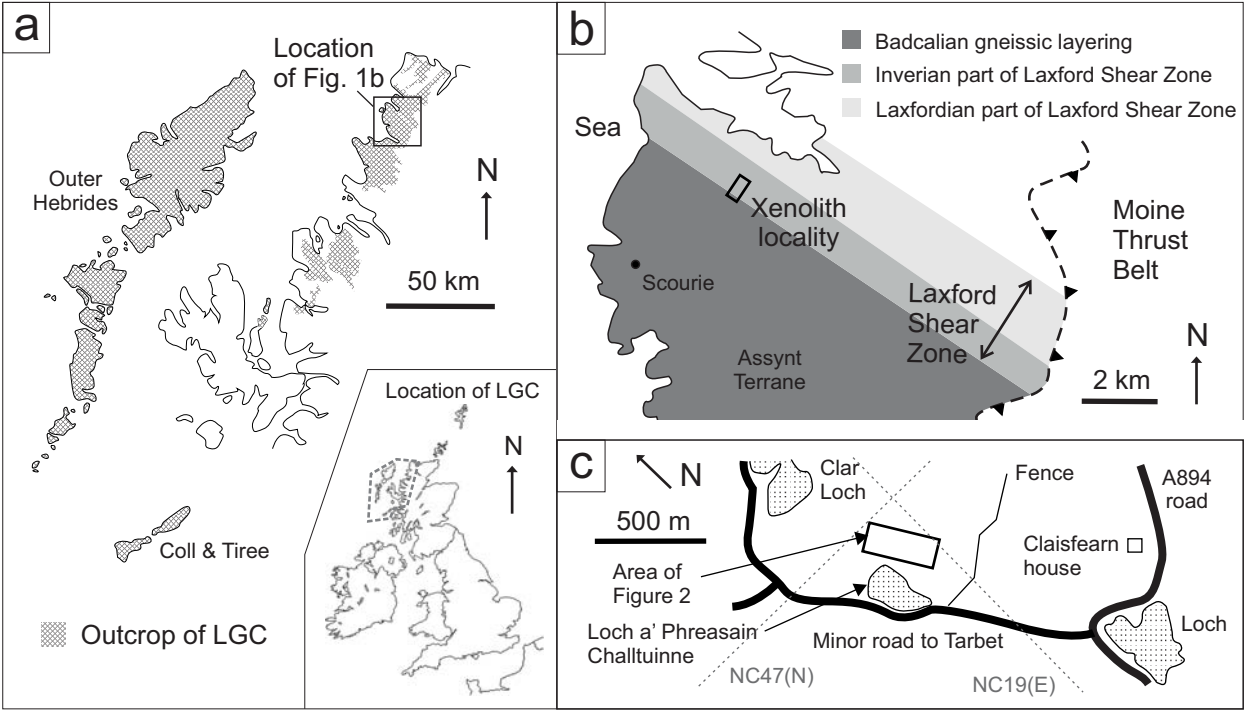
a
Location of Fig. 1b
Outer Hebrides
N
50 km
Location of LGC
N
Coll & Tiree
Outcrop of LGC
b
Badcalian gneissic layering
Inverian part of Laxford Shear Zone
Laxfordian part of Laxford Shear Zone
Sea
Xenolith locality
Scourie
Moine Thrust Belt
Laxford Shear Zone
Assynt Terrane
N
2 km
c
N
500 m
Clar Loch
Fence
A894 road
Claisfearn house
Area of Figure 2
Loch a' Phreasain Challtuinne
Minor road to Tarbet
Loch
NC47(N)
NC19(E)

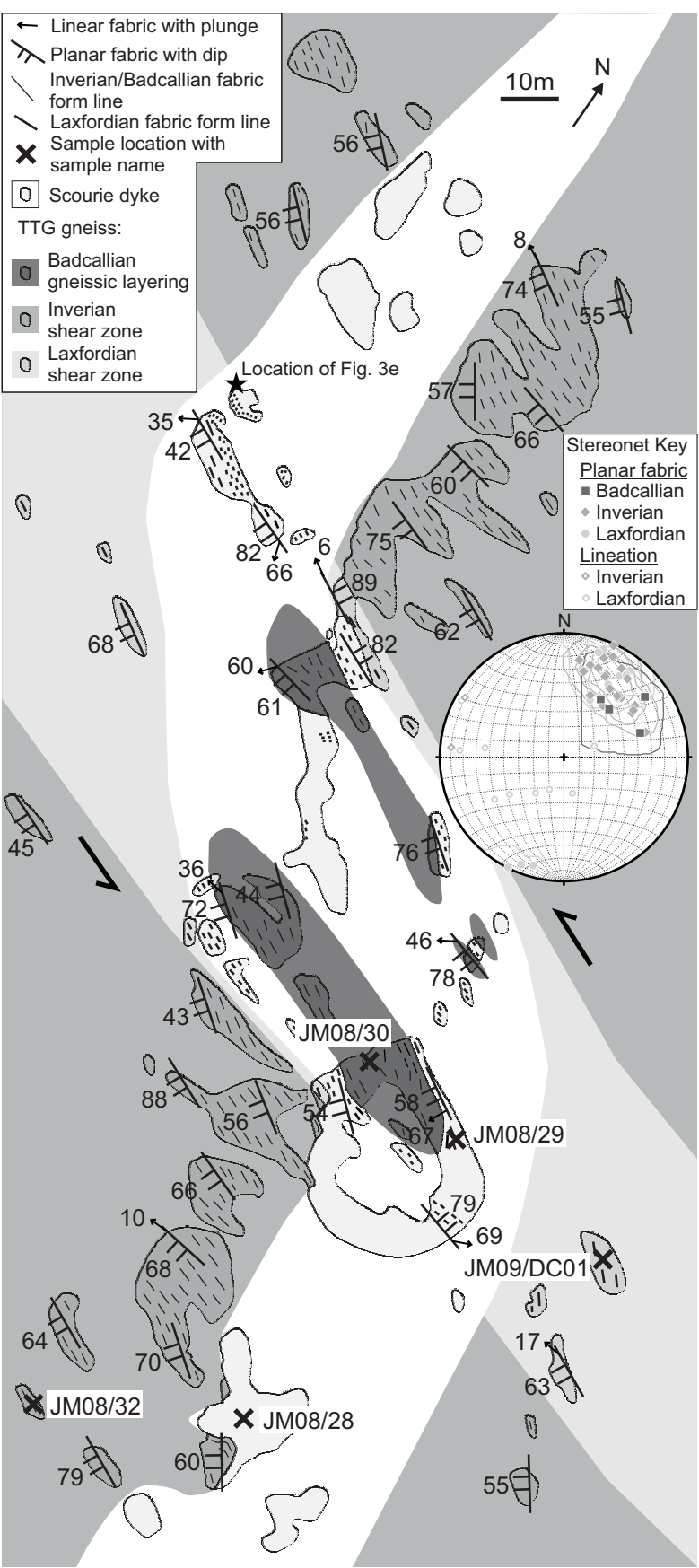
Linear fabric with plunge
Planar fabric with dip
Inverian/Badcallian fabric form line
Laxfordian fabric form line
Sample location with sample name
Scourie dyke
TTG gneiss:
Badcallian gneissic layering
Inverian shear zone
Laxfordian shear zone
10m
N
Location of Fig. 3e
Stereonet Key
Planar fabric
Badcallian
Inverian
Laxfordian
Lineation
Inverian
Laxfordian
JM08/30
JM08/29
JM09/DC01
JM08/28
JM08/32
56
56
8
74
55
57
66
35
42
60
82
66
6
75
89
68
82
62
60
61
45
76
36
44
72
46
78
43
88
56
54
58
67
66
79
10
68
69
64
70
17
63
79
60
55

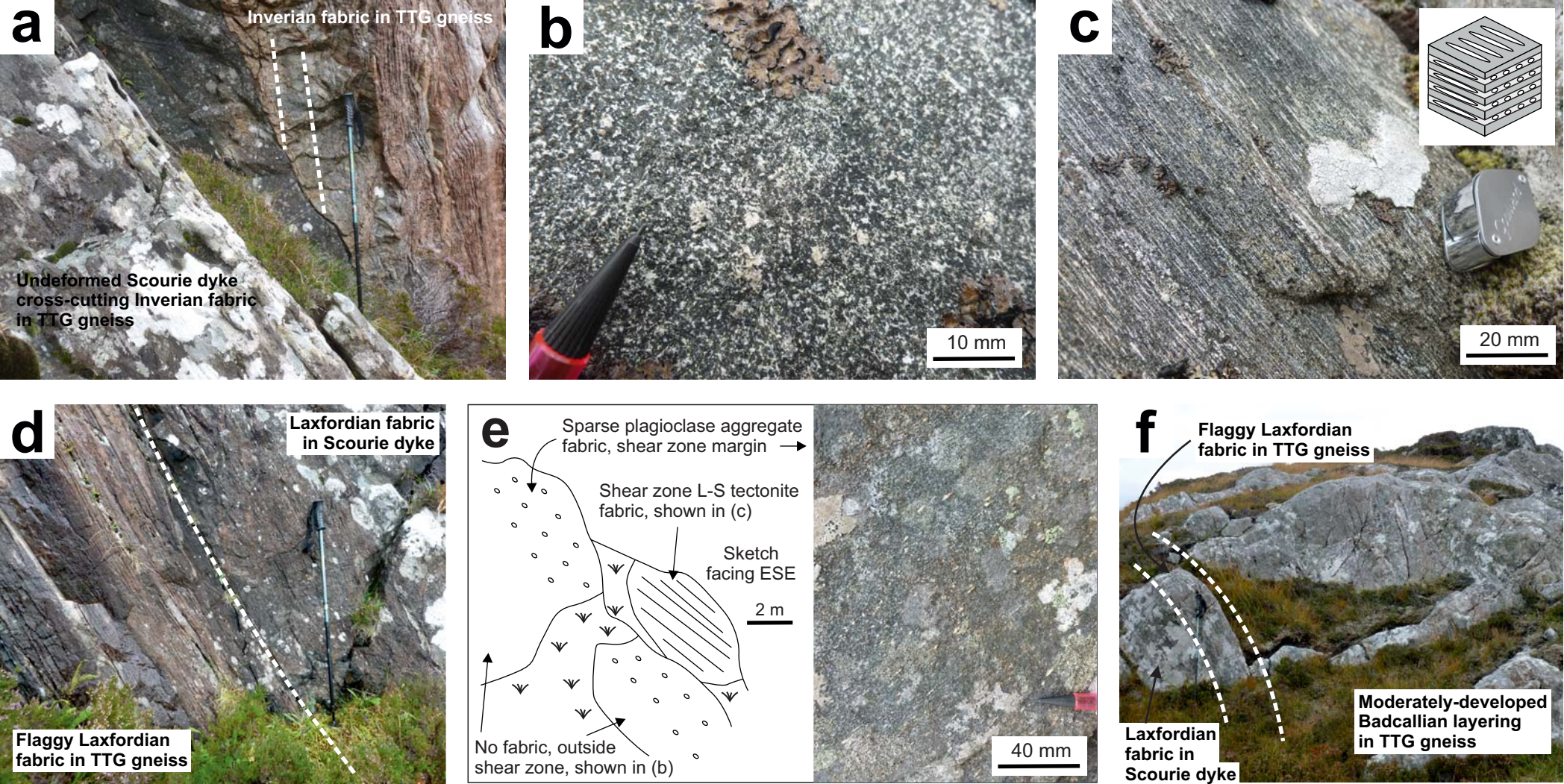
a
Inverian fabric in TTG gneiss
Undeformed Scourie dyke cross-cutting Inverian fabric in TTG gneiss
b
10 mm
c
20 mm
d
Laxfordian fabric in Scourie dyke
Flaggy Laxfordian fabric in TTG gneiss
e
Sparse plagioclase aggregate fabric, shear zone margin
Shear zone L-S tectonite fabric, shown in (c)
Sketch facing ESE
2 m
No fabric, outside shear zone, shown in (b)
40 mm
f
Flaggy Laxfordian fabric in TTG gneiss
Laxfordian fabric in Scourie dyke
Moderately-developed Badcallian layering in TTG gneiss

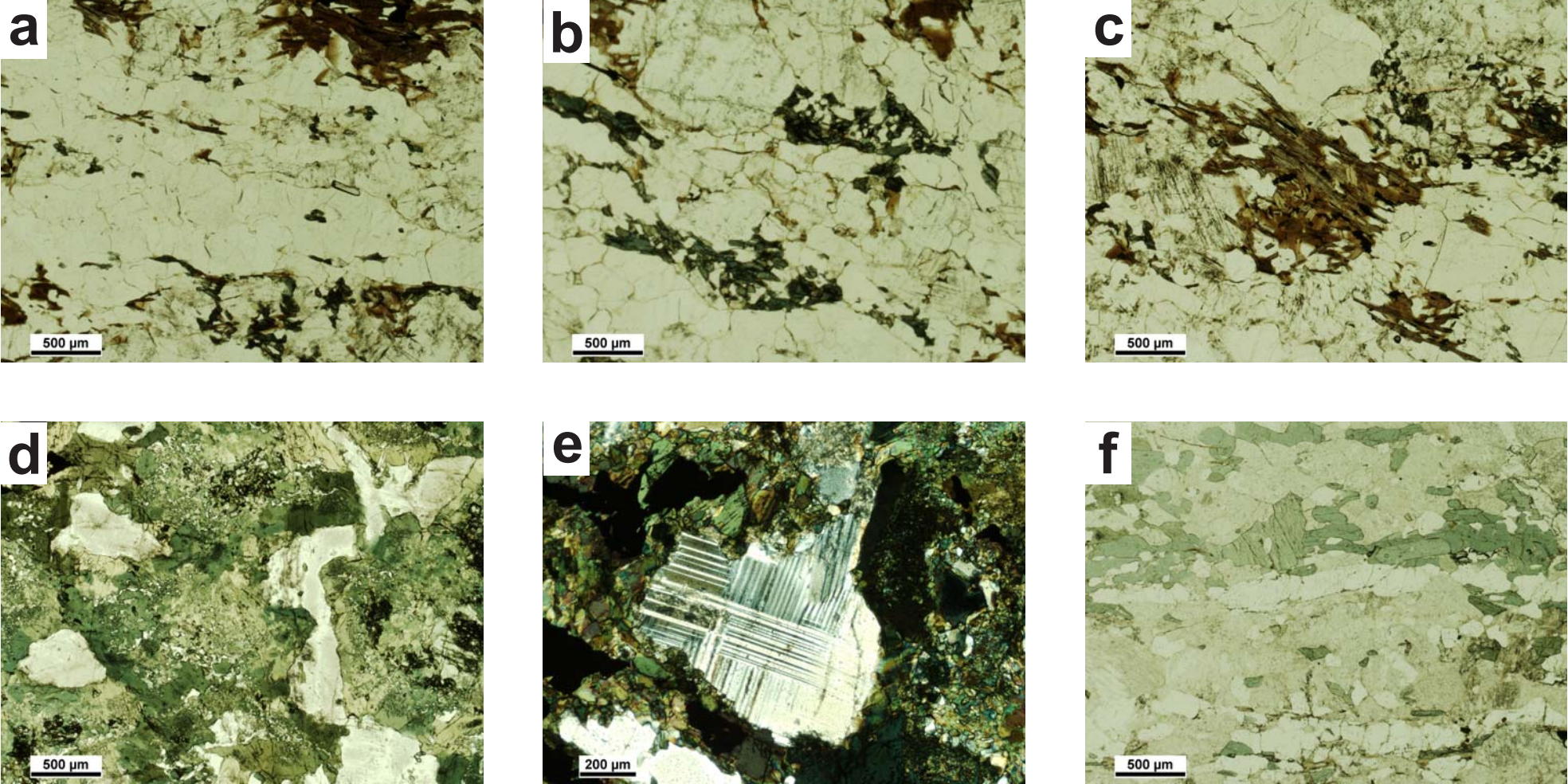
a
500 µm
b
500 µm
c
500 µm
d
500 µm
e
200 µm
f
500 µm

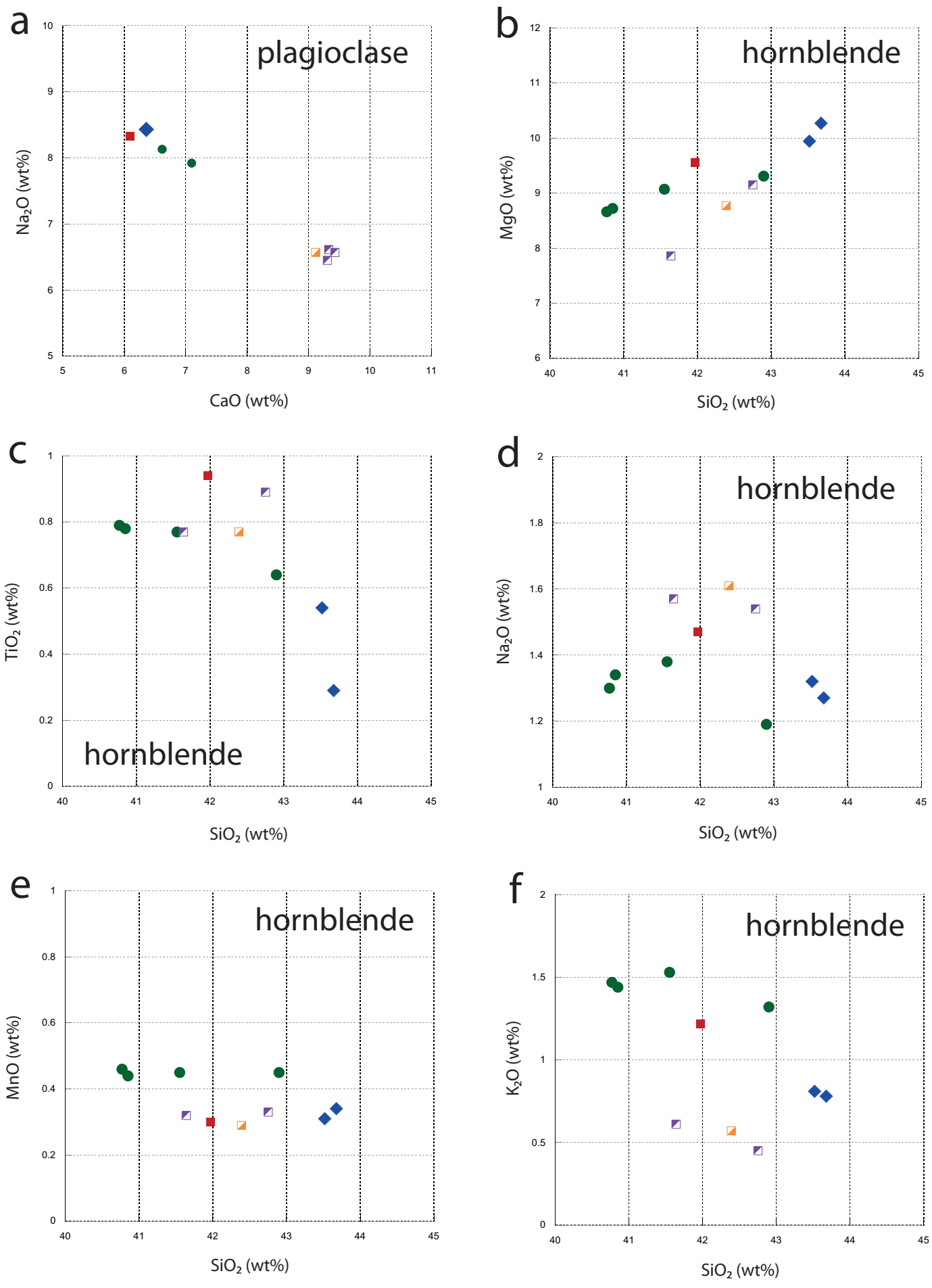

- JM08/28 - undefomed Scourie Dyke
- JM08/29 - defomed Scourie Dyke
- JM08/30 - TTG gneiss from xenolith in Scourie Dyke (hornblendes are narrow rims around clinopyroxenes)
- JM09/DC01 - TTG gneiss with Laxfordian fabric (hornblende is fabric-forming lath)
- JM08/32 - TTG gneiss with Inverian fabric (hornblendes are sieve-textured)

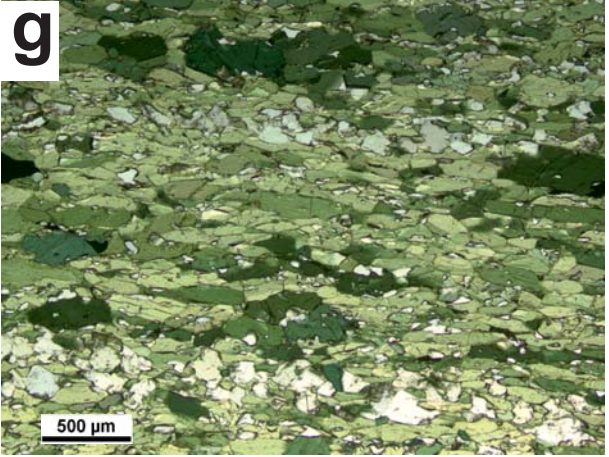
g
500 µm

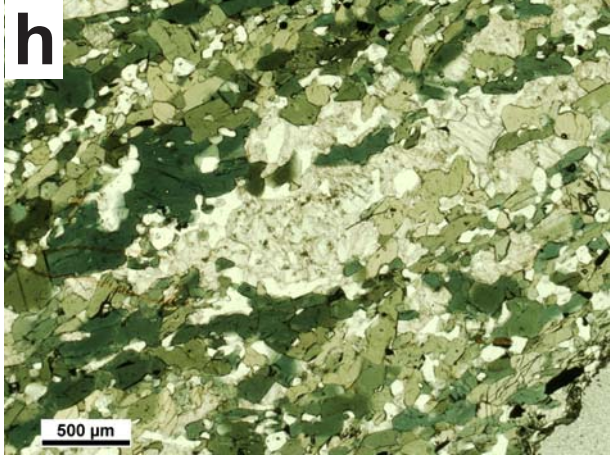
h
500 µm

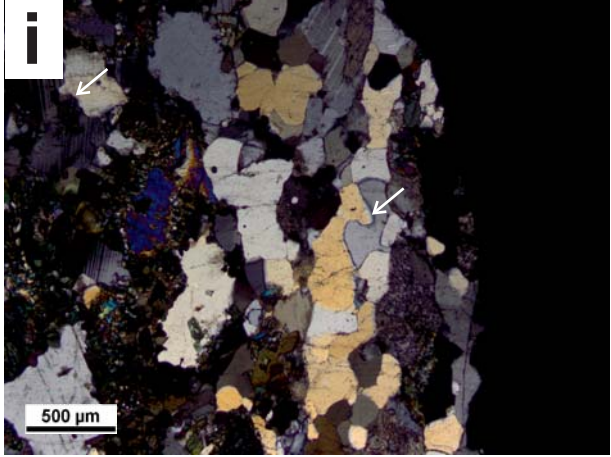
i
500 µm

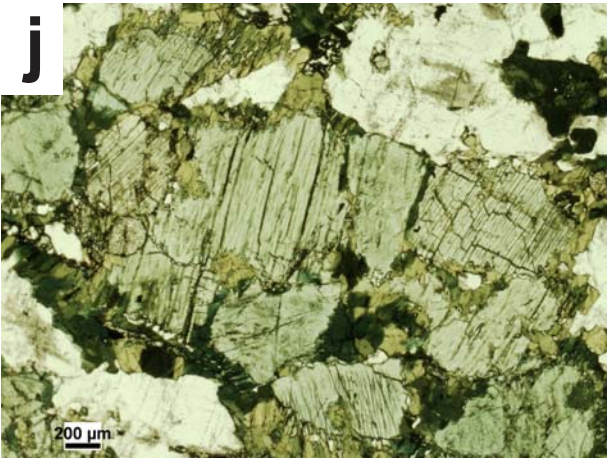
j
200 µm

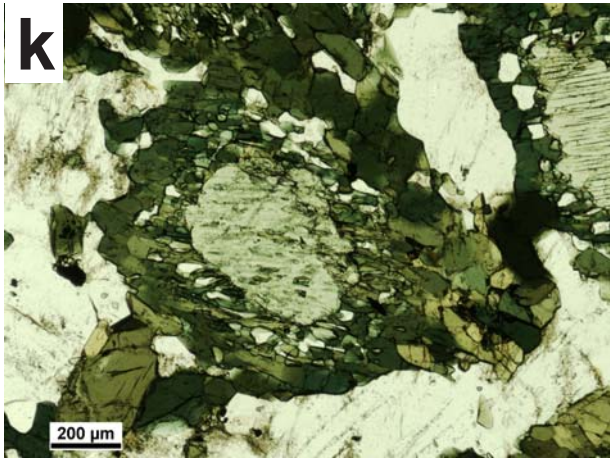
k
200 µm

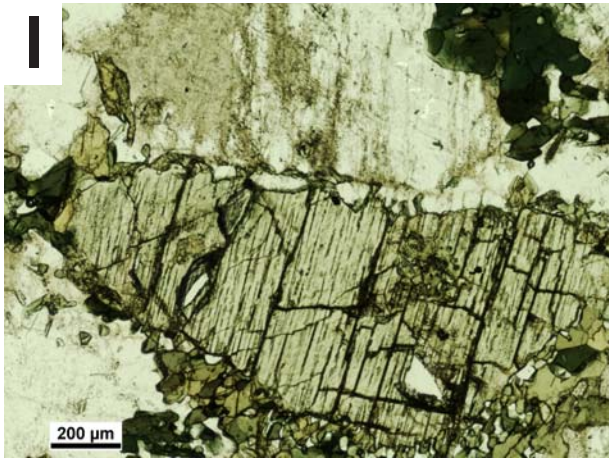
l
200 µm

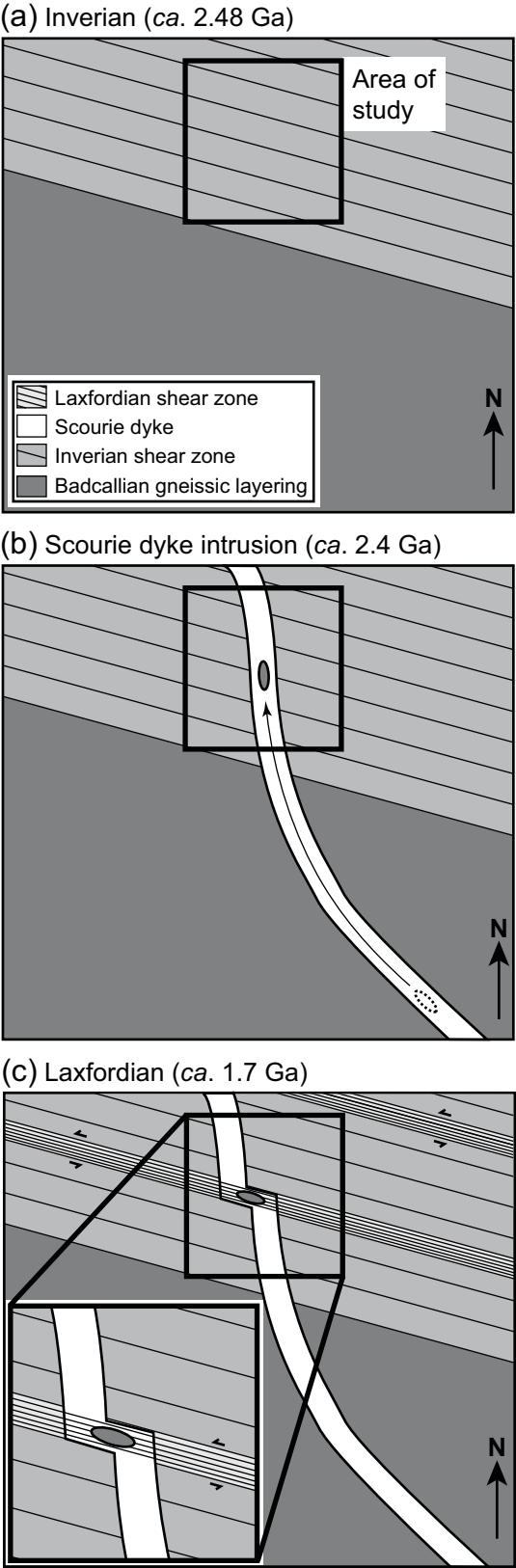
(a) Inverian (ca. 2.48 Ga)
Area of study
Laxfordian shear zone
Scourie dyke
Inverian shear zone
Badcallian gneissic layering
N
(b) Scourie dyke intrusion (ca. 2.4 Ga)
N
(c) Laxfordian (ca. 1.7 Ga)
N